ELSEVIER

Journal of Molecular Catalysis B: Enzymatic 8 (2000) 85–94

JOURNAL OF MOLECULAR CATALYSIS B: ENZYMATIC

www.elsevier.com/locate/molcatb

Development of the active site model for calcium-containing quinoprotein alcohol dehydrogenases

Shinobu Itoh *, Hirokatsu Kawakami, Shunichi Fukuzumi [1]

Department of Material and Life Science, Graduate School of Engineering, Osaka University, 2-1 Yamada-oka, Suita, Osaka 565-0871, Japan

Dedicated to: Professor Johannis A. Duine for his excellent achievements, great contribution, and leadership in the progress of the chemistry and enzymology of quinoproteins

Abstract

A new PQQ model compound [dimethyl 7-(1,4,7,10-tetraoxa-13-azacyclopentadec-13-yl)carbonyl-4,5-dihydro-4,5-dioxo-1*H*-pyrrolo[2,3-*f*]quinoline-2,9-dicarboxylate, **1**], in which a 1-aza-15-crown-5 group is attached through an amide linkage at the 7-position, has been synthesized in order to develop an efficient model system of calcium-containing quinoprotein alcohol dehydrogenases. It has been found that Ca^{2+} binds to the quinone most strongly among the alkaline earth metal ions examined ($Ca^{2+} + > Sr^{2+} + \gg Ba^{2+} + \gg Mg^{2+}$) and the binding constant (K_M) for Ca^{2+} is as large as 2.1×10^5 M^{-1}. Formation of the C-5 hemiacetal derivatives with ethanol is also investigated spectrophotometrically to show that the alcohol-addition to the quinone is enhanced in the presence of the metal ions. In this case, Ca^{2+} and Sr^{2+} show a similar efficiency that is several times larger than that of Ba^{2+}. Addition of a strong base such as DBU (1,8-diazabicyclo[5.4.0]undec-7-ene) into a MeCN solution containing the metal ion complex of **1** and ethanol leads to redox reactions to give the Ca^{2+} complex of $\mathbf{1H_2}$ (quinol form) and acetaldehyde. Kinetic studies on the redox reactions have been performed to gain insight into the mechanism of the alcohol-oxidation reaction catalyzed by the metal complexes of coenzyme PQQ.

Keywords: Calcium-containing quinoprotein alcohol dehydrogenase; Active site model; Coenzyme PQQ

1. Introduction

Quinoprotein alcohol dehydrogenases (E.C. 1.1.99.8) comprise a new class of enzymes that involve a heterocyclic *o*-quinone coenzyme PQQ (4,5-dihydro-4,5-dioxo-1*H*-pyrrolo[2,3-*f*]-quinoline-2,7,9-tricarboxylic acid, pyrroloquinolinequinone) as a redox catalyst for the enzymatic alcohol-oxidation reactions (Eq. (1)) [1].

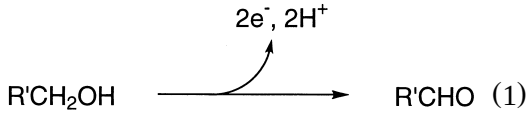

(1)

The recent X-ray crystallographic analysis of quinoprotein methanol dehydrogenases (MDH) from methylotrophic bacteria has provided full particulars of the enzyme active center to show that there is one calcium ion strongly bound to

* Corresponding author.
[1] Also corresponding author.

1381-1177/00/$ - see front matter
PII: S1381-1177(99)00070-3

PQQ through its C-5 quinone carbonyl oxygen, N-6 pyridine nitrogen, and C-7 carboxylate group in the enzyme active site [2,3]. Existence of Ca^{2+} in the enzyme active site has also been suggested for other PQQ-dependent enzymes such as ethanol dehydrogenase from *Pseudomonas aeruginosa* and glucose dehydrogenase from *Acinetobacter calcoaceticus* [4,5]. Harris and Davidson [6] have recently suggested that Ca^{2+} plays an important role for the structural stabilization of the enzyme, but little is known about the catalytic role of Ca^{2+} for the redox reaction of the enzymes [7]. In this context, we have recently succeeded in demonstrating that the calcium complex of PQQ can oxidize methanol to formaldehyde in anhydrous organic media [8]. On the basis of detailed kinetic analysis using a series of PQQ model compounds, we proposed the addition–oxidative elimination mechanism through the C-5 hemiacetal intermediate as shown in Scheme 1 [9]. In this reaction sequence, Ca^{2+} facilitates the alcohol-addition to the quinone and stabilizes the hemiacetal intermediate thus formed. It has also been suggested that the base-catalyzed α-proton abstraction from the added substrate is enhanced by the complex formation with Ca^{2+} [9]. In order to develop more efficient model system, we herein synthesized a new PQQ model compound (**1**) in which a 1-aza-15-crown-5 group is attached through an amide linkage at the 7-position and examined its M^{2+}-binding ability and reactivity in the alcohol-oxidation reaction (M^{2+} denotes alkaline earth metal ion). So far, coenzyme engineering and functionalization have not only provided valuable information about enzymatic mechanisms and functions but has also been used to develop artificial enzymes and catalysts [10].

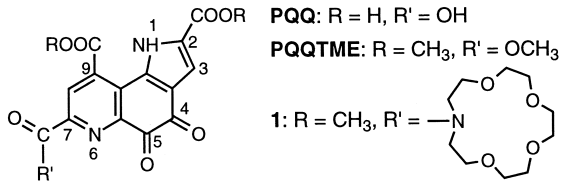

2. Experimental

All the chemicals used in this study were commercial products of the highest available purity and were further purified by the standard methods, if necessary [11]. All alkaline earth metal ions used in this study were obtained as ClO_4^- salts. UV-vis spectra were recorded on a Hewlett Packard 8452A or a Hewlett Packard 8453 photo diode array spectrophotometer. Mass spectra were recorded with a JEOL JNX-DX303 HF mass spectrometer or a Shimadzu GCMS-QP2000 gas chromatograph mass spectrometer. ^1H NMR and ^{13}C NMR spectra were obtained on a JEOL FT-NMR EX-270 spectrometer. Molecular orbital calculations were performed with the PM3 method by using a Spartan program (Version 4.1, Wavefunction). Final geometries and energetics were obtained by optimizing the total molecular energies with respect to all structural variables.

*2.1. Synthesis of model compound **1***

Dimethyl 5-methoxy-7-(1,4,7,10-tetraoxa-13-azacyclopentadec-13-yl)-carbonyl-1*H*-pyrrolo-[2,3-*f*]quinoline-2,9-dicarboxylate (**4**): Model

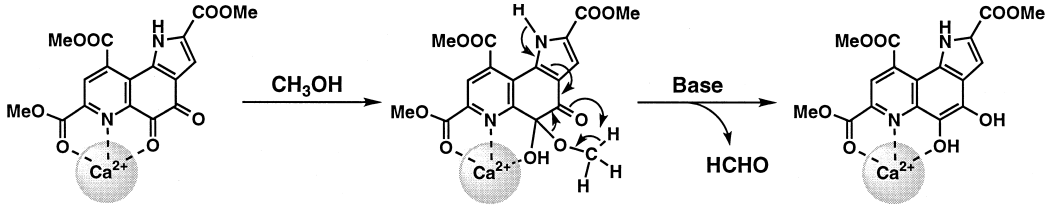

Scheme 1.

compound **1** has been synthesized by applying a reported procedure [12] from trimethyl 5-methoxy-1*H*-pyrrolo[2,3-*f*]quinoline-2,7,9-tricarboxylate (**2**, a synthetic intermediate of the total synthesis of coenzyme PQQ [13]). Thus, the regioselective ester hydrolysis of **2** (100 mg, 0.27 mmol) in CF_3COOH/H_2O (2:1, 5 ml) at 60°C for 24 h provided 2,9-dimethyl ester 7-carboxy derivative **3** [12] to which 1-aza-15-crown-5 was introduced by acid chlorination with $(COCl)_2$ (1.7 mmol) in C_6H_6 (3 ml) at a refluxing temperature for 24 h, and the following reaction with 1-aza-15-crown-5 (10 eq) in CH_2Cl_2 (4 ml) at room temperature for additional 24 h. Amide derivative **4** was isolated by flash column chromatography (SiO_2, AcOEt:EtOH = 4:1) in a 43% yield (63.3 mg) from **2**. ^{1}H NMR (270 MHz, TMS, CD_3Cl) δ 3.63–3.89 (m, 20H, $-CH_2CH_2-$), 4.00 (s, 3H, $-OCH_3$), 4.08 (s, 3H, $-OCH_3$), 4.13 (s, 3H, $-OCH_3$), 7.29 (d, 1H, $J = 2.4$ Hz, 3-H), 7.33 (s, 1H, 4-H), 8.63 (s, 1H, 8-H), 12.1 (bs, 1H, 1-H); IR (KBr disk) 3340 (NH, OH), 1722 (ester C=O), 1632 (amide C=O), 1258 (ether C–O) cm^{-1}; HRMS m/z 559.2126 calcd. for $C_{27}H_{33}O_{10}N_3$ 559.2166.

Dimethyl 7-(1,4,7,10-tetraoxa-13-azacyclopentadec-13-yl)carbonyl-4,5-dihydro-4,5-dioxo-1*H*-pyrrolo[2,3-*f*]quinoline-2,9-dicarboxylate (**1**): Oxidation of **4** (50.8 mg, 0.091 mmol) with 5 eq of ceric ammonium nitrate (CAN, 0.47 mmol) in $MeCN/H_2O$ (4/1, 2.5 ml) at 0°C for 10 min and following purification by flash column chromatography (SiO_2, AcOEt: EtOH = 4:1) afforded an expected *o*-quinone **1** in a 60% isolated yield. ^{1}H NMR (270 MHz, TMS, CD_3Cl) δ 3.67–3.84 (m, 20H, $-CH_2CH_2-$), 3.97 (s, 3H, $-OCH_3$), 4.13 (s, 3H, $-OCH_3$), 7.46 (d, 1H, $J = 2.2$ Hz, 3-H), 8.46 (s, 1H, 8-H), 12.9 (bs, 1H, 1-H); IR (KBr disk) 3224 (NH, OH), 1722 (ester C=O), 1686 (quinone C=O), 1628 (amide C=O), 1234 (ether C–O) cm^{-1}; HRMS m/z 559.1803 calcd. for $C_{27}H_{29}O_{11}N_3$ 559.1804; Anal. calcd. for $C_{27}H_{29}O_{11}N_3$ C 55.03, H 5.15, N 7.40, found: C 54.93, H 5.32, N 7.39.

2.2. Titration

The binding constants (K_M) for the 1:1-complex formation between the quinone (2.5×10^{-5} M) and alkaline earth metal ions (Mg^{2+}, Ca^{2+}, Sr^{2+}, and Ba^{2+}) were determined by spectrophotometric titration using a 1 cm path length UV cell in anhydrous MeCN at 25°C using Eq. (2). The data are summarized in Table 1.

The equilibrium constants (K_{add}) for the alcohol-addition to the quinone (2.5×10^{-5} M) were determined in the presence and absence of the metal ion by spectrophotometric titration using a 1-cm path length UV cell in anhydrous MeCN at 25°C. The metal ion concentrations used in the titrations were large enough to convert all the quinone to the corresponding metal complexes. The analytical procedure has been already reported in the literature [14].

2.3. Kinetic analysis

Oxidation of ethanol by the metal complexes of **1** was followed by UV-vis spectra under pseudo-first-order conditions with excess ethanol in deaerated MeCN at 25°C. Typically, an anhydrous MeCN solution containing **1** (2.5×10^{-5} M), $Ca(ClO_4)_2$ and EtOH was placed in a UV

Table 1
Metal ion binding constants (K_M) and UV/Vis absorption maxima (λ_{max}) in MeCN

Quinone	Ionic radius[a]		λ_{max}, nm		K_M, M^{-1} [b]
	M^{2+}	Å	Quinone	$[M(\mathbf{Q})]^{2+}$	
1	Mg^{2+}	0.66	352	–[d]	72
1	Ca^{2+}	0.99	352	364	210000
1	Sr^{2+}	1.12	352	364	110000
1	Ba^{2+}	1.34	352	364	40000
PQQTME[c]	Mg^{2+}	0.66	354	–[d]	< 5
PQQTME[c]	Ca^{2+}	0.99	354	368	1900
PQQTME[c]	Sr^{2+}	1.12	354	366	590
PQQTME[c]	Ba^{2+}	1.34	354	365	380

[a] Taken from Handbook of Chemistry and Physics, 61st edn., CRC Press, Boca Raton, 1981.
[b] The experimental error is within ±5%.
[c] The data are taken from the literature [9].
[d] The λ_{max} value could not be determined accurately because of the following hydration reaction of the quinone moiety.

cell (1-cm path length, sealed tightly with a silicon rubber cap) and was deaerated by bubbling Ar through it for ca. 20 min. Then deaerated DBU (1,8-diazabicyclo[5.4.0]undec-7-ene) was added with a microsyringe to start the reaction. The pseudo-first-order rate constant (k_{obs}) was calculated from the rate of the decrease in intensity of the absorption due to the quinone or the increase in intensity of the absorption due to the product. The Mac curve fit program (version 1.0) was used for the non-linear curve fitting of the plots of k_{obs} vs. [EtOH] and of k_{obs} vs. [DBU] to obtain the kinetic parameters (K_a, K_{add}, and k). The data are summarized in Table 2.

2.4. Product analysis

The oxidation product, acetaldehyde, was isolated as the 2,4-dinitrophenylhydrazone derivative, and its yield was determined by ^{1}H NMR (in $CDCl_3$). Formation of the 2,4-dinitrophenylhydrazone of acetaldehyde was confirmed by comparing the peaks of the product to those of an authentic sample, and its yield was determined by using tetrachloroethane as an internal reference.

Table 2
Kinetic parameters for the oxidation of ethanol by $[M(\mathbf{1})]^{2+}$ and $[M(PQQTME)]^{2+}$ in MeCN[a]

Quinone	M^{2+}	K_{add}, M^{-1} [b,c]	k, M^{-1} s^{-1} [b]	K_a, M^{-1} [b]
1	Ca^{2+}	1.0 (1.2)	1.7	0.99×10^3
1	Sr^{2+}	1.5 (1.5)	58	3.4×10^3
1	Ba^{2+}	0.38 (0.38)	2800	5.5×10^3
PQQTME[d]	Ca^{2+}	1.1 (1.2)	2.1	1.0×10^3
PQQTME[d]	Sr^{2+}	0.79 (0.79)	39	2.6×10^3
PQQTME[d]	Ba^{2+}	0.41 (0.41)	150	5.0×10^3

[a] Obtained from the plots of k_{obs} vs. [ROH].
[b] The experimental error is within $\pm5\%$.
[c] The K_{add} values determined by the titration are shown in parentheses.
[d] The data are taken from the literature [9].

3. Results and discussion

3.1. Synthesis

Model compound **1** has been synthesized by applying a reported procedure [12] from trimethyl 5-methoxy-1*H*-pyrrolo[2,3-*f*]quinoline-2,7,9-tricarboxylate (**2**). Thus, the regioselective ester hydrolysis of **2** in CF_3COOH/H_2O (2:1) at 60°C for 24 h provided 2,9-dimethyl ester 7-carboxy derivative (**3**) to which 1-aza-15-crown-5 was introduced by acid chlorination with $(COCl)_2$ and the following reaction with 1-aza-15-crown-5. After purification by flash column chromatography (SiO_2), CAN oxidation of the resulting material **4** afforded an expected *o*-quinone **1**.

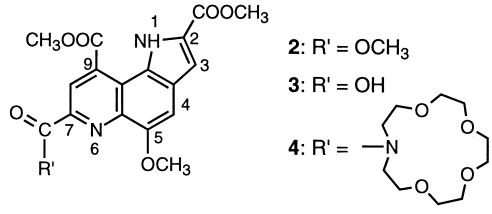

3.2. Metal ion coordination

The trimethyl ester of coenzyme PQQ (PQQTME) has been shown to bind Ca^{2+} with the binding constant $K_M = 1.9\times10^3$ M^{-1} in the same place as PQQ in the enzyme; a molecular cleft surrounded by the quinone carbonyl group at C-5 (O-5), the pyridine nitrogen (N-6), and the carboxyl group at the 7-position (O-7′) [8,9]. Addition of $Ca(ClO_4)_2$ to **1** in anhydrous acetonitrile (MeCN) at 25°C gave us a similar spectral change as that observed in the titration of PQQTME with $Ca(ClO_4)_2$ under the same experimental conditions. The absorption band at 352 nm due to the quinone shifted to 364 nm and the absorption band at 278 nm decreased with an increase at 260 nm with clear isosbestic points as shown in Fig. 1. The binding constant K_M for 1:1-complex formation between the

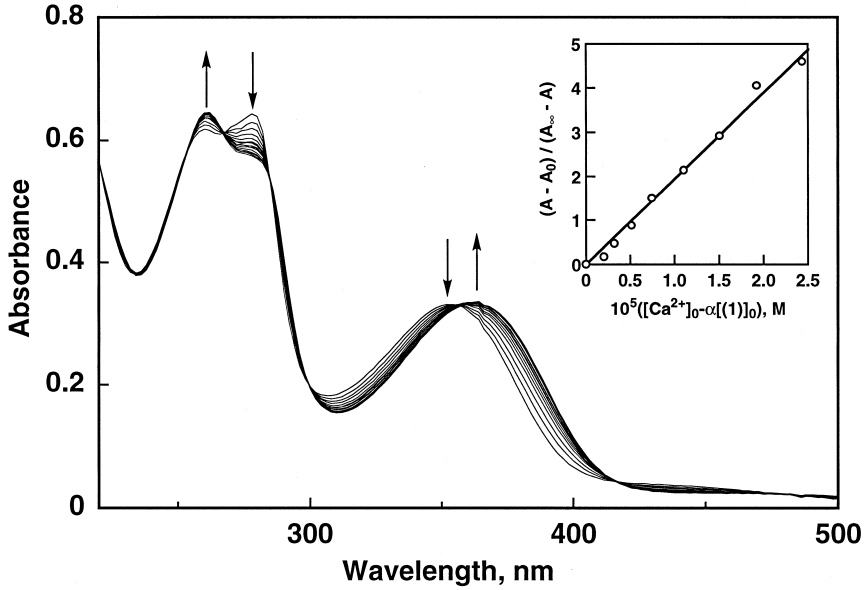

Fig. 1. Spectral change observed upon addition of $Ca(ClO_4)_2$ (0–1.9×10^{-4} M) to a MeCN solution of **1** (2.5×10^{-5} M) at 25°C. Inset: plot of $(A - A_0)/(A_\infty - A)$ vs. $[Ca(ClO_4)_2]_0 - \alpha[\mathbf{1}]_0$ $[\alpha = (A - A_0)/(A_\infty - A_0)]$ for the Ca^{2+}-complex formation of **1**.

quinone (Q) and the metal ion (M^{2+}) can be determined by Eq. (2),

$$\frac{A - A_0}{A_\infty - A} = K_M\left([M^{2+}]_0 - \frac{A - A_0}{A_\infty - A_0}[Q]_0\right) \quad (2)$$

where A_0 and A_∞ are the initial and final absorptions of the titration, and $[M^{2+}]_0$ and $[Q]_0$ denote the concentration of the added metal ion and the initial quinone concentration, respectively. Thus, the plot of $(A - A_0)/(A_\infty - A)$ vs. $([Ca^{2+}]_0 - \alpha[\mathbf{1}]_0)$ $[\alpha = (A - A_0)/(A_\infty - A_0)]$ gave a straight line passing through the origin as shown in the inset of Fig. 1, from which $K_M = 2.1 \times 10^5$ M^{-1} was obtained as the slope.

In spite of our great efforts, a single crystal of the Ca^{2+} complex of **1** suitable for the X-ray analysis could not be obtained. However, the ^1H and ^{13}C NMR data in MeCN-d_3 clearly indicate that the binding position of Ca^{2+} to **1** in acetonitrile is the same as that to PQQTME as follows. In the ^1H NMR spectra, the methylene protons of the crown ring moved down field by the complexation with Ca^{2+} ($\Delta\delta$ = ca. +0.2) and the $\Delta\delta$ (down-field shift by the complexation) value of H-8 is larger than that of H-3 (+0.22 and +0.06, respectively). In the ^{13}C NMR spectra, down-field shifts of C-5 and C-7′ (amide carbonyl carbon at the 7-position) were relatively large (Δppm = +2.9 and +5.0, respectively), while the chemical shifts of C-4, C-2′ (ester carbonyl carbon at the 2-position), and C-9′ (ester carbonyl carbon at the 9-position) were very small (Δppm = −0.5, +0.4, and −0.4, respectively). Essentially, the tendencies of the chemical shifts in the ^1H and ^{13}C NMR and of the UV/Vis spectral change were the same as those obtained in the titration with PQQTME, indicating that the interaction between Ca^{2+} and the quinone moiety takes place at the same positions; the C-5 quinone carbonyl oxygen and the N-6 pyridine nitrogen.

In Fig. 2 is shown a computer generated structure of the Ca^{2+} complex of **1** using a Spartan program (version 4.1). The calcium ion has a hepta-coordinate geometry with the O(5′)N(6)N(amide)4O(crown) donor set, where all Ca^{2+}–O distances are 2.376 ± 0.008 Å and the distances of Ca^{2+}–N(6) and Ca^{2+}–N(amide)

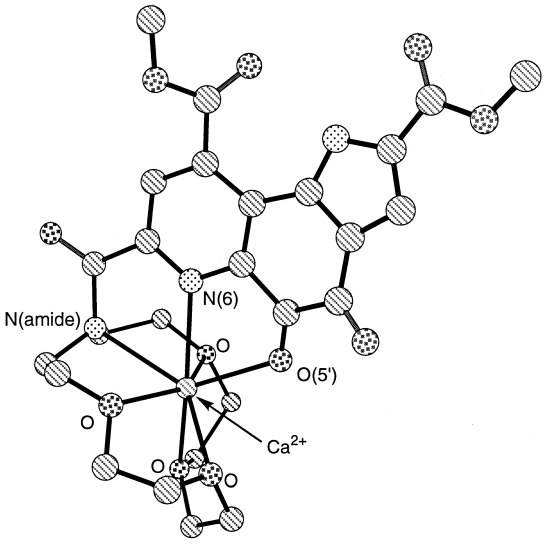

Fig. 2. Chem3D representation of the optimized structure of $[Ca(\mathbf{1})]^{2+}$ by Spartan (version 4.1). All hydrogen atoms are omitted for clarity.

are 2.498 Å and 2.580 Å, respectively. These values of the atom distances are fairly close to those in the enzyme (Ca^{2+}–O(5): 2.50 Å, Ca^{2+}–N(6): 2.47 Å, Ca^{2+}–O(7′): 2.30 Å) [2] and are within the range of the reported values for Ca^{2+}–O=C and Ca^{2+}–N_{py} distances in crystals (see the reference papers cited in Ref. [9]), indicating that Ca^{2+} fits perfectly in the metal binding site as designed by us. The larger K_M value of **1** as compared to PQQTME (more than two-orders of magnitude) can be attributed to the good fitting of Ca^{2+} into the metal binding pocket of **1**.

Essentially the same spectral changes (bathochromic shift of the absorption band at 352 nm and decrease of the one at 278 nm) were obtained in the titrations of **1** with Mg^{2+}, Sr^{2+}, and Ba^{2+} (Table 1), implying that the binding position of these metal ions to **1** is essentially the same. The K_M values of **1** to the metal ions were then determined by analyzing the spectral changes in a similar manner described above, and they are listed in Table 1 together with the λ_{max} of the quinone and its metal complexes.

Incorporation of the crown ether ring into the PQQ molecule significantly enhances the metal ion binding ability, and the K_M value reached the order of 10^5 M^{-1} in the case of Ca^{2+} and Sr^{2+}. It should be also noted that the binding of Ca^{2+} to the quinone is the strongest among the alkaline earth metal ions examined. It is probably due to the best fitting of Ca^{2+} to the metal binding site comprised of O(5′), N(6), and the crown ether ring as indicated by the computer simulation (Fig. 2). Binding of the larger metal ions such as Sr^{2+} and Ba^{2+} would induce some strain around the metal binding site and Mg^{2+} may be too small to bring the quinone moiety and the crown ether ring together.

3.3. Hemiacetal formation

Addition of ethanol into a MeCN solution of $[Ca(\mathbf{1})]^{2+}$ resulted in a spectral change shown in Fig. 3 which indicates C-5 hemiacetal formation. The equilibrium constant K_{add} for the hemiacetal formation of $[Ca(\mathbf{1})]^{2+}$ with ethanol was determined as 1.2 M^{-1} by the titration (inset of Fig. 3) as listed in Table 2. The K_{add} value thus determined is six times larger than that measured in the absence of Ca^{2+} (K_{add} = 0.20 M^{-1}). The enhancing effect of Ca^{2+} for the hemiacetal formation of $[Ca(\mathbf{1})]^{2+}$ with ethanol is exactly the same as that observed for that of PQQTME with ethanol (K_{add} = 0.20 M^{-1} for PQQTME and K_{add} = 1.2 M^{-1} for $[Ca(PQQTME)]^{2+}$) [9], indicating clearly that there is no inhibiting effect such as steric hindrance by the crown ether ring on the alcohol-addition reaction. Almost the same K_{add} value (1.5 M^{-1}) was obtained for $[Sr(\mathbf{1})]^{2+}$, but that value became smaller (0.38 M^{-1}) for $[Ba(\mathbf{1})]^{2+}$. The smaller K_{add} value of $[Ba(\mathbf{1})]^{2+}$ as compared to those of $[Ca(\mathbf{1})]^{2+}$ and $[Sr(\mathbf{1})]^{2+}$ can be attributed to its larger ion size which may induce some strain in the resulting C-5 hemiacetal derivative. Such a smaller effect of Ba^{2+} than Ca^{2+} was also observed in the addition of ethanol to PQQTME [9].

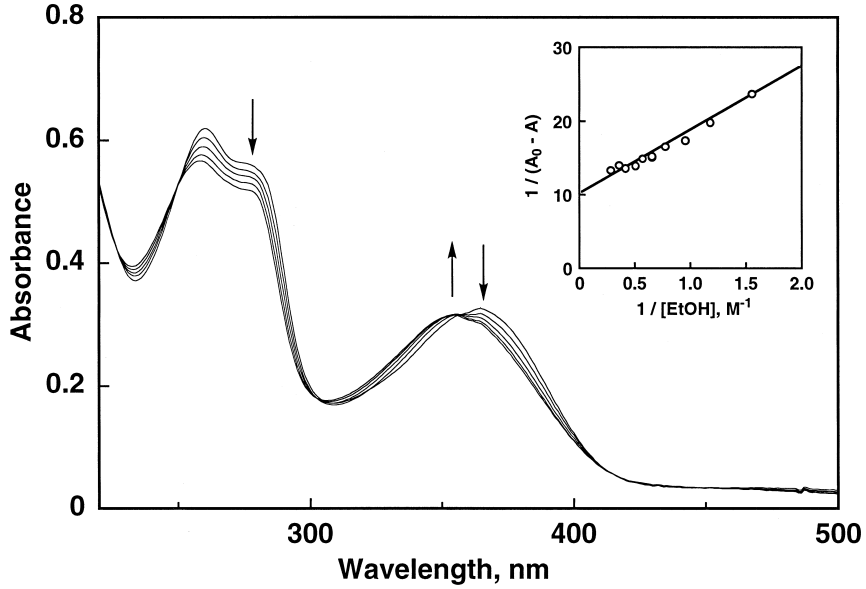

Fig. 3. Spectral change after the reaction of **1** (2.5×10^{-5} M) with EtOH (0–3.5 M) in the presence of $Ca(ClO_4)_2$ (1.1×10^{-4} M) in MeCN at 25°C. Inset: Plot of $1/(A - A_0)$ vs. $1/[EtOH]$ for the titration of **1** in the presence of $Ca(ClO_4)_2$ with EtOH.

3.4. Base-catalyzed alcohol-oxidation

Addition of ethanol into a deaerated MeCN solution containing $[Ca(\mathbf{1})]^{2+}$ and a strong base such as DBU (1,8-diazabicyclo[5.4.0]undec-7-ene) resulted in reduction of the quinone to the corresponding quinol ($\mathbf{1H_2}$). In Fig. 4 is shown a spectral change of the reaction at 25°C in

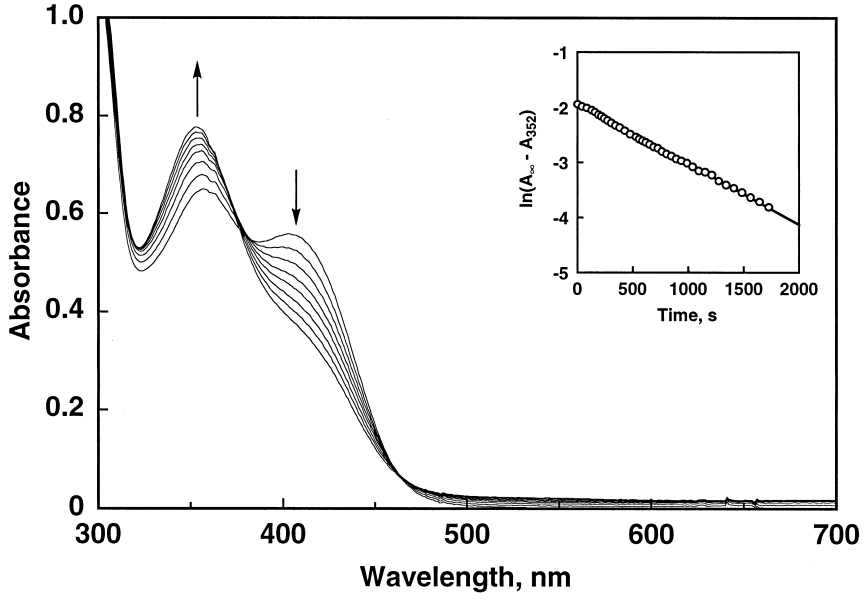

Fig. 4. Spectral change observed during the oxidation of EtOH (1.0 M) by **1** (5.5×10^{-5} M) in the presence of $Ca(ClO_4)_2$ (1.1×10^{-4} M) and DBU (1.6×10^{-3} M) in deaerated MeCN at 298 K. Inset: Pseudo-first-order plot based on the absorption change at 352 nm due to the quinone.

MeCN under anaerobic conditions. The final spectrum of the reaction mixture is very close to that obtained by the treatment of authentic PQQTMEH$_2$ (quinol form [15]) with $Ca(ClO_4)_2$ and DBU in deaerated MeCN. From the reaction mixture on a preparative scale ([**1**] = 1.3×10^{-4} M, $[Ca(ClO_4)_2] = 1.3 \times 10^{-4}$ M, [DBU] = 2.4×10^{-3} M, [EtOH] = 1.5 M in 100 ml of MeCN), acetaldehyde was isolated quantitatively as the 2,4-dinitrophenylhydrazone derivative.

A first-order plot for the rate of formation of the reduced product is shown in the inset of Fig. 4. The pseudo-first-order rate constant (k_{obs}) thus obtained shows a Michaelis–Menten type saturation dependence with respect to the ethanol concentration as indicated in Fig. 5A. Non-linear curve fitting using Eq. (3),

$$k_{obs} = kK_{add}[EtOH][DBU]/(1 + K_a[DBU] + K_{add}[EtOH]) \quad (3)$$

derived from the reaction mechanism shown in Scheme 2 provided the kinetic parameters as $K_a = 0.99 \times 10^3$ M^{-1}, $K_{add} = 1.0$ M^{-1}, and $k = 1.7$ M^{-1} s^{-1}, where K_a is the deprotonation equilibrium constant ($\mathbf{1}^-$ represents deprotonated quinone at N-1) and k is the rate constant of the oxidative elimination of the product from $[Ca(\mathbf{1}_{OEt})]^{2+}$ to produce $[Ca(\mathbf{1H_2})]^{2+}$ and MeCHO. The dependence of k_{obs} vs. [DBU] (Fig. 5B) also afforded a similar saturation phenomenon as expected from the kinetic Eq. (3), from which $K_a = 1.1 \times 10^3$ M^{-1}, $K_{add} = 1.1$ M^{-1}, and $k = 1.7$ M^{-1} s^{-1} were obtained by the computer simulation. The good agreements of those kinetic parameters determined independently from k_{obs} vs. [EtOH] and k_{obs} vs. [DBU] together with the agreement of K_{add} determined by the titration (1.2 M^{-1}) and kinetics (1.0 M^{-1} and 1.1 M^{-1}) support the validity of the proposed addition–elimination mechanism.

The kinetic parameters (K_{add}, k, and K_a) for the oxidation of ethanol by $[Sr(\mathbf{1})]^{2+}$ and by $[Ba(\mathbf{1})]^{2+}$ were obtained in the same procedures and they are summarized in Table 2. In all cases, the K_{add} values determined independently from the plots of k_{obs} vs. [ROH] agree well with those determined by the titrations of the metal ion complexes of **1** with ethanol. Thus, the oxidation of these alcohols proceeds via the same addition–base catalyzed elimination mechanism through the C-5 hemiacetal intermediate (Scheme 2).

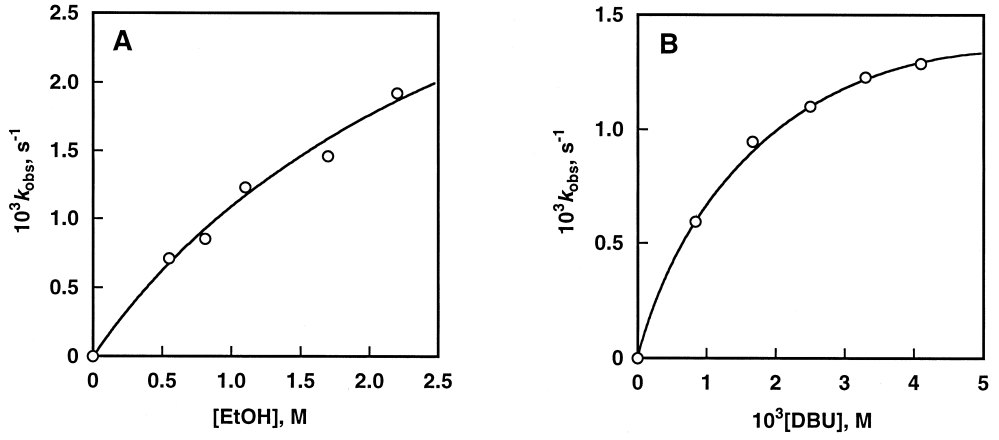

Fig. 5. Plots of (A) k_{obs} vs. [EtOH] for the oxidation of EtOH by **1** (2.5×10^{-5} M) in the presence of $Ca(ClO_4)_2$ (1.1×10^{-4} M) and DBU (3.3×10^{-3} M), and (B) k_{obs} vs. [DBU] for the oxidation of EtOH (1.1 M) by **1** (2.5×10^{-5} M) in the presence of $Ca(ClO_4)_2$ (1.1×10^{-4} M) and DBU in deaerated MeCN at 25°C.

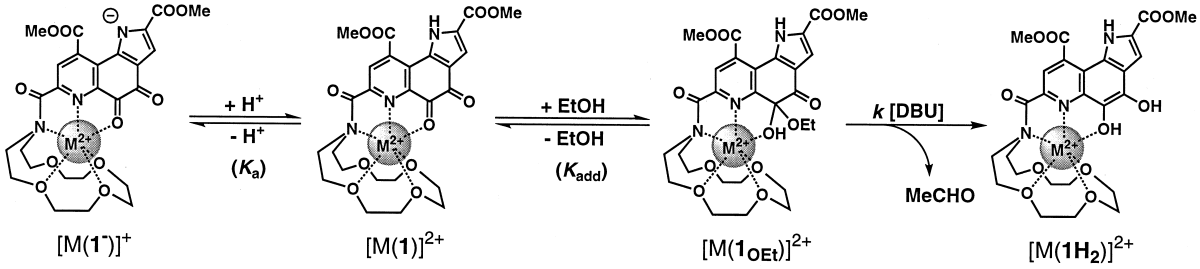

Scheme 2.

Inspection of Table 2 clearly indicates that the catalytic effect of the metal ions on the alcohol-addition process (K_{add}) and the acid–base equilibrium (K_a) of the pyrrole proton are basically the same between **1** and PQQTME, while the acceleration of the oxidative elimination process (k) by the larger ions ($Ba^{2+} > Sr^{2+} > Ca^{2+}$) is more pronounced in the case of **1** as compared to PQQTME. The larger catalytic effect of the larger metal ions on the oxidative elimination process (k) has been explained by taking account of the intramolecular general-base catalysis by the C-4 carbonyl oxygen (Scheme 3) [9]. Namely, the binding of larger metal ions such as Ba^{2+} and Sr^{2+} to the hemiacetal of PQQ forces the added alcohol moiety closer to the C-4 quinone carbonyl oxygen than in the case of Ca^{2+}, making the α-proton abstraction by the carbonyl oxygen easier. Such a pushing effect of the added alcohol moiety by the larger ions may be further enhanced by the incorporated crown ether group from the back (Scheme 3).

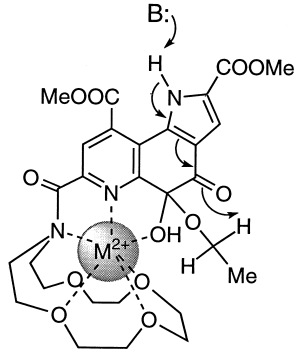

Scheme 3.

In summary, we have developed a new synthetic model for the active site of quinoprotein alcohol dehydrogenases, where the binding of alkaline earth metal ions and the catalytic effects of the metal ions on the alcohol-addition (K_{add}) and the base-catalyzed oxidative elimination processes (k) have been explored. Introduction of a 1-aza-15-crown-5 group into the 7-position of the PQQ molecule resulted in essentially the same spectral changes (UV/Vis and ^1H and ^{13}C NMR) as a result of complex formation with alkaline earth metal ions as in the case of PQQTME, and increased the metal ion binding ability by ca. two orders of magnitude as compared with that of PQQTME. These results gave us further evidence that the metal ion binding site in the model system is the same as that observed in the enzyme. Kinetic studies on ethanol oxidation by **1** also gave us further evidence for the addition–elimination mechanism. The order of the catalytic efficiency on the alcohol-addition step (K_{add}) is $Ca^{2+} = Sr^{2+} > Ba^{2+}$ and that on the base-catalyzed elimination process (k) is $Ca^{2+} < Sr^{2+} < Ba^{2+}$, which are similar to those of the enzymatic system (V_{max} and K_m) [16]. In the present system with **1**, the difference of the catalytic efficiencies of M^{2+} in the base-catalyzed elimination process (k) is much more pronounced as compared to the system with PQQTME itself (see Table 2). This can be explained by taking account of the intramolecular general-base catalysis by the C-4 carbonyl oxygen in the α-proton abstraction of the added substrate as discussed above (Scheme 3).

During the initial submission of this article, Zheng and Bruice [17] reported the theoretical studies on the catalytic role of Ca^{2+} in quinoprotein MDH. They pointed out the possibility of a hydride transfer mechanism from calcium methoxide to C-4 quinone carbonyl oxygen of PQQ. In our model reactions, however, formation of the C-5 hemiacetal intermediate has been undoubtedly demonstrated by the spectroscopic analysis and the detailed kinetic investigations. As one may argue, the hydride transfer mechanism which involves the C-5 hemiacetal derivative as a bystander in a side-equilibrium is kinetically indistinguishable from the proposed addition–elimination mechanism involving the C-5 hemiacetal as the real active species. In the theoretical calculations, however, they also demonstrated that both the direct hydride transfer and the addition–elimination mechanisms go through a same transition state to give formaldehyde and reduced PQQ, clearly suggesting that the C-5 hemiacetal could not be the nonproductive intermediate in a side-equilibrium. Thus, it can be concluded that their calculation results support validity of our proposed addition–elimination mechanism for the present model reaction.

Acknowledgements

The present study was financially supported in part by a Grant-in-Aid for Scientific Research on Priority Area (Molecular Biometallics, 08249223 and 09235218) and a Grant-in-Aid for General Scientific Research (08458177) from the Ministry of Education, Science, Sports, and Culture of Japan.

References

[1] J.A. Duine, Eur. J. Biochem. 200 (1991) 271.
[2] Z.-x. Xia, W.-w. Dai, Y.-f. Zhang, S.A. White, G.D. Boyd, F.S. Mathews, J. Mol. Biol. 259 (1996) 480.
[3] M. Ghosh, C. Anthony, K. Harlos, M.G. Goodwin, C. Blake, Structure 3 (1995) 177.
[4] A. Mutzel, H. Görisch, Agric. Biol. Chem. 55 (1991) 1721.
[5] O. Geiger, H. Görisch, Biochem. J. 261 (1989) 415.
[6] T.K. Harris, V.L. Davidson, Biochem. J. 303 (1994) 141.
[7] C. Anthony, Biochem. J. 320 (1996) 697.
[8] S. Itoh, H. Kawakami, S. Fukuzumi, J. Am. Chem. Soc. 119 (1997) 439.
[9] S. Itoh, H. Kawakami, S. Fukuzumi, Biochemistry 37 (1998) 6562.
[10] H. Dugas, Bioorganic Chemistry, Chap. 7, 3rd edn., Springer, Berlin, 1996.
[11] D.D. Perrin, W.L.F. Armarego, D.R. Perrin, Purification of Laboratory Chemicals, Pergamon, Elmsford, NY, 1966.
[12] S. Itoh, T. Inoue, Y. Fukui, X. Huang, M. Komatsu, Y. Ohshiro, Chem. Lett. (1990) 1675.
[13] E.J. Corey, A. Tramontano, J. Am. Chem. Soc. 103 (1981) 5599.
[14] S. Itoh, M. Ogino, Y. Fukui, H. Murao, M. Komatsu, Y. Ohshiro, T. Inoue, Y. Kai, N. Kasai, J. Am. Chem. Soc. 115 (1993) 9960.
[15] S. Itoh, Y. Ohshiro, T. Agawa, Bull. Chem. Soc. Jpn. 59 (1986) 1911.
[16] M.G. Goodwin, C. Anthony, Biochem. J. 318 (1996) 673.
[17] Y. Zheng, T.C. Bruice, Proc. Natl. Acad. Sci. U.S.A. 94 (1997) 11881.